



Deposited via The University of Leeds.

White Rose Research Online URL for this paper:

<https://eprints.whiterose.ac.uk/id/eprint/87124/>

Version: Accepted Version

Article:

Austin, L, Liskiewicz, T, Kolev, I et al. (2015) The influence of anti-wear additive ZDDP on doped and undoped diamond-like carbon coatings. *Surface and Interface Analysis*, 47 (7). 755 - 763. ISSN: 0142-2421

<https://doi.org/10.1002/sia.5763>

Reuse

Items deposited in White Rose Research Online are protected by copyright, with all rights reserved unless indicated otherwise. They may be downloaded and/or printed for private study, or other acts as permitted by national copyright laws. The publisher or other rights holders may allow further reproduction and re-use of the full text version. This is indicated by the licence information on the White Rose Research Online record for the item.

Takedown

If you consider content in White Rose Research Online to be in breach of UK law, please notify us by emailing eprints@whiterose.ac.uk including the URL of the record and the reason for the withdrawal request.

The Influence of Antiwear Additive ZDDP on Doped and Undoped Diamond-Like Carbon Coatings.

Austin, L*¹, Liskiewicz, T¹, Kolev, I², Zhao, H¹, Neville, A.¹

¹ Institute of Functional Surfaces, School of Mechanical Engineering, University of Leeds, Leeds, UK

² Hauzer Techno Coating, Venlo, Netherlands

Abstract

Diamond-like carbon (DLC) coatings are recognised as a promising way to reduce friction and improve wear performance of automotive engine components. DLC coatings provide new possibilities in the improvement of the tribological performance of automotive components beyond what can be achieved with lubricant design alone. Lubricants are currently designed for metallic surfaces, the tribology of which is well defined and documented. DLC does not share this depth of tribological knowledge; thus, its practical implementation is stymied. In this work, three DLC coatings are tested: an amorphous hydrogenated DLC, a silicone-doped amorphous hydrogenated DLC and a tungsten-doped amorphous hydrogenated DLC. The three coatings are tested tribologically on a pin-on-reciprocating plate tribometer against a cast iron pin in a group III base oil, and a fully formulated oil that consists of a group III base oil and contains ZDDP, at 100 °C for 6 h and for 20 h in order to determine whether a phosphor-based tribofilm is formed at the contact. The formation of a tribofilm is characterised using atomic force microscopy and X-ray photoelectron spectroscopy techniques. The main findings of this study are the formation of a transfer film at the un-doped, amorphous hydrogenated DLC surface, and also the tungsten amorphous hydrogenated DLC having a significant wear removal during the testing. The three coatings were found to have differing levels of wear, with the tungsten-doped DLC showing the highest, the silicon-doped DLC showing some coating removal and the amorphous hydrogenated DLC showing only minimal signs of wear

1. Introduction

Diamond-Like Carbon (DLC) coatings are gaining an increasing prevalence within many industries, including biomedical [1-4], automotive components (for both racing and select production vehicles) [3, 5-7] and magnetic storage media (further improved tribological properties) [3, 4, 8, 9]. The reasons for this interest are their low friction and low wear capabilities in tribologically demanding areas. Many review papers throughout the past few decades have been focussed on DLC coatings from the mid-80s –90s [10-13], to the early 2000s [14-17] and more recently [1, 5].

There is an increasing demand on automotive car engine manufacturers to find more innovative and environmentally sustainable technologies for passenger vehicle engines. Low friction and wear coatings for this purpose are being developed, and must be compatible with existing lubricants within the engine in order to be economically viable. DLC could be the solution to this problem; however, one question which has yet to be answered is whether DLC is compatible with existing engine lubricants. In this paper, the common anti-wear additive ZDDP will be used in order to determine if a tribofilm derived from this additive is formed.

Some authors have found a ZDDP derived tribofilm [18-20] and some have found no stable tribofilm on the DLC surface [21, 22], rather that it was formed on the counter body and transferred to the DLC during sliding. This study focuses on three types of DLC coating, one amorphous hydrogenated diamond like carbon (a-C:H), a silicon doped DLC (Si-DLC), both of which were deposited at the University of Leeds, and a W-doped DLC (W-DLC) which is a Oerlikon Balzers Balanit C* coating. The coatings are characterised mechanically and chemically, using nano-indentation, atomic force microscopy (AFM), transmission electron microscopy (TEM), electron energy loss spectroscopy (EELS). X-ray photoelectron spectroscopy (XPS), white light interferometry and AFM was used in order to characterise tribofilms on the surface of the DLC.

2. Experimental Methodology

2.1. Experimental Details

The materials used in these experiments were as follows: for the substrates used to deposit the DLC, an M2 bearing grade steel was used, and for the counter body, a cast iron pin with curvature of 40 mm was used. The lubrication regime was boundary. This and the entrainment speed detailed in section 2.1.1 were chosen in order to represent those experienced by a cam follower in a passenger car vehicle. The a-C:H and Si-DLC were both deposited on a Hauzer Flexicoat 850 PECVD and PVD deposition rig, using acetylene as the hydrocarbon source and Hexamethyldisiloxane as the Si precursor for the Si-DLC.

2.1.1. Tribological Experiments

A pin-on-reciprocating-plate tribometer was used to evaluate the tribological performance of three DLC coatings; a schematic of this can be seen in figure 2-1. The frictional force was measured using a bi-directional load cell calibrated before the experiment. The friction force data was recorded every 5 minutes for 2 seconds in each of the tests. The tests were carried out for 6 and 20 hours and were repeated at least three times. Before the tests, the samples were cleaned in an ultrasonic bath in acetone for 15 minutes. Lubricant was added to the sample holder (4 ml) and brought to 100 °C before the test began. Two lubricants were selected for this study: (i) a group III base oil, and (ii) a fully formulated European group III base oil incorporating ZDDP additive and other species such as detergents, dispersants and antioxidants. The average linear speed during the tests was 0.015 ms^{-1} and the applied stroke was 10 mm. A load of 281 N was applied to the samples by a cast iron pin, with 40 mm radius of curvature, which corresponds to a Hertzian contact pressure of 750 MPa.

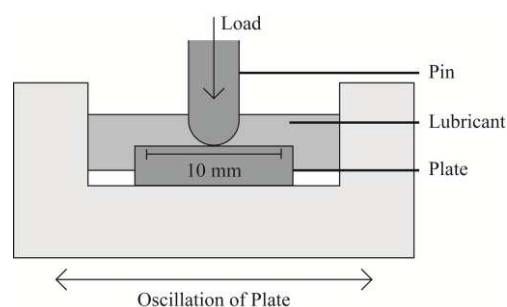


Figure 2-1: A schematic of the pin-on-reciprocating plate tribometer

2.1.2. Wear Analysis

The total wear volume of the wear scar created by the tribological testing was determined using an optical white light interferometer. Dimensional wear coefficients corresponding to the wear rates were calculated by inputting the volume loss into Archard's wear equation:

$$V = kFs \quad 1$$

Where: V is the wear volume (m^3), k is the dimensional wear coefficient per unit load and per unit distance ($\text{m}^3\text{N}^{-1}\text{m}^{-1}$), F is the normal load (N) and s is the sliding distance (m).

2.1.3. Hardness and Elastic Modulus

The coating hardness was measured using a nano-indentation platform (Micromaterials Nano-Test Platform) with a Berkovich type indenter. Measurements of the load-displacement curves were conducted at a load of 1 mN, these were then analysed using the Oliver and Pharr method [23]. The elastic modulus was calculated using equation 2 from the value of reduced modulus (E_r) given by the software.

$$\frac{1}{E_r} = \frac{(1 - \nu_s^2)}{E_s} + \frac{(1 - \nu_i^2)}{E_i} \quad 2$$

Where E_r is the reduced modulus, ν_i and E_i are the poisson's ratio (0.07) and elastic modulus (1141 GPa) of the indenter tip, respectively, ν_s and E_s are the poisson's ratio and the elastic modulus of the specimen, respectively.

The indenter and maximum load were chosen to ensure that the maximum penetration depth of the indentation was no more than 10% of the coating with a loading/unloading rate of 2 mN/min. A minimum of ten indentations was carried out on each sample.

2.1.4. TEM and EELS

Focussed ion beam transmission electron microscope (FIBTEM) sections were prepared from the samples using an FEI Nova 200 Nanolab dual beam scanning electron microscope, fitted

with a Kleindiek micromanipulator. The ion column was operated at 30 kV and 5 kV, at beam currents between 5 nA and 0.05 nA and the electron column at 5 kV and 29 pA. The site of interest was coated in a 200 nm platinum layer in order to protect the surface. The surrounding material was removed using a gallium ion beam, and the finished section removed using the micromanipulator and attached to the TEM sample grid. The section was thinned to < 100 nm in order to be useful within the TEM. The TEM and EELS were carried out using a Philips CM200 FEGTEM operated at 197 keV. The EEL spectra were fitted according to Daniels et al [24].

2.1.5. XPS

The chemical analysis of the tribofilms was carried out using a VG ESCALAB 250 X-ray Photoelectron Spectrometer (XPS) using high power monochromatized x-ray of aluminium K alpha source, high transmission electron optics and a multi-channel detector. An area of 500 μm x 500 μm was analysed in the wear scar region. A survey was carried out at a pass energy of 150 eV at first to determine which elements were present. Longer scans at 20 eV pass energy of the selected peaks were then obtained to gain a clearer picture of the chemical composition. CASAXPS software was used to analyse the data. The position of the C1s peak at 285 eV was used as the reference point for charge correction found in an XPS handbook [25]. The peak area ratio, full width at half maximum (FWHM) and difference between binding energies of the doublets were constrained. The processed data within this study has taken into account a linear or curved background approximation and is deemed appropriate for the comparison of the tribofilm formation between samples. The samples were rinsed for 10s in n-heptane prior to experimentation to remove any residual oils or contaminating species.

3. Results

3.1. Mechanical properties

The hardness and elastic modulus for the coatings tested in this section are presented in table 3-1. The H/E ratio is hypothesised to be a measure of the wear resistance of the coating, this has been recognised by several authors as being in very close agreement to a materials wear

resistance [26] i.e. the higher the H/E ratio of a coating, the higher the maximum tensile elastic stress is predicted to be [27], and can correspond with a higher wear resistance, this will be investigated within this work. The H/E ratios for the a-C:H, a-C:H:Si and W-DLC samples are presented in table 3-1.

As can be seen from the results in table 3-1, the a-C:H is substantially harder than the W-DLC and slightly harder than Si-DLC. Although it is only ~ 3 GPa harder than the Si, the elastic modulus of the a-C:H is significantly higher, suggesting that the Si inclusion in the DLC matrix lowers this value. The W-DLC has a high elastic modulus and a low hardness when compared to the Si-DLC.

Table 3-1: Hardness, elastic modulus and H/E ratio of the coatings

Sample	Hardness (GPa)	Elastic Modulus (GPa)	H/E
a-C:H	31.1 ± 1.5	262.4 ± 24.8	0.12
Si-DLC	27.8 ± 1	188.6 ± 7.4	0.15
W-DLC	16.8 ± 2.7	161.4 ± 23.3	0.10

3.2. TEM and EELS

TEM samples were prepared from each of the coatings, figure 3-1 shows an example of curve fitting of an EELS spectrum of a-C:H. Three peaks are fitted in accordance with [24]. The percentage of sp^2 bonding is determined by comparing the ratio of the π^* peak to the total area, to the value of this found from pure graphite. This was done for each of the samples, a-C:H, a-C:H:Si and W-DLC and the results of which are presented in figure 3-2.

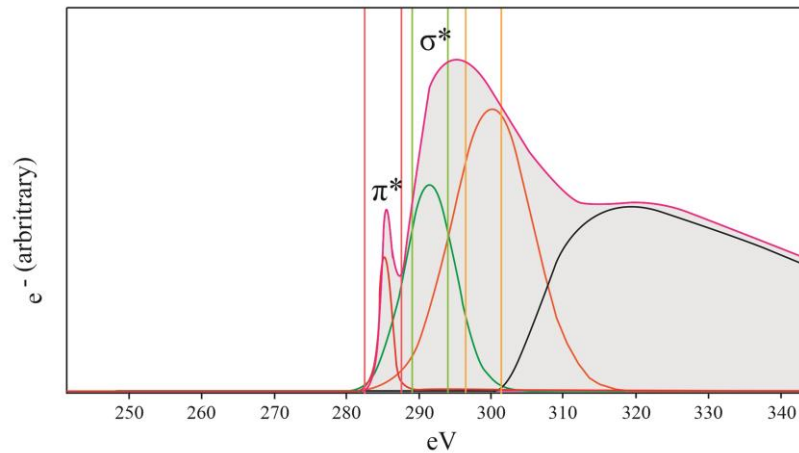


Figure 3-1: Example of the curve fit to an electron energy loss spectroscopy spectra using the a-C:H sample

The percentage of sp^2 is highest in the a-C:H coating, this was unexpected as it was also the hardest of the three coatings tested. The lowest sp^2 was found in the Si-DLC, followed by the W-DLC. This does not necessarily mean that there is a higher percentage of sp^3 bonding in these coatings, as there could be other types due to there being Si or W incorporated into the coatings.

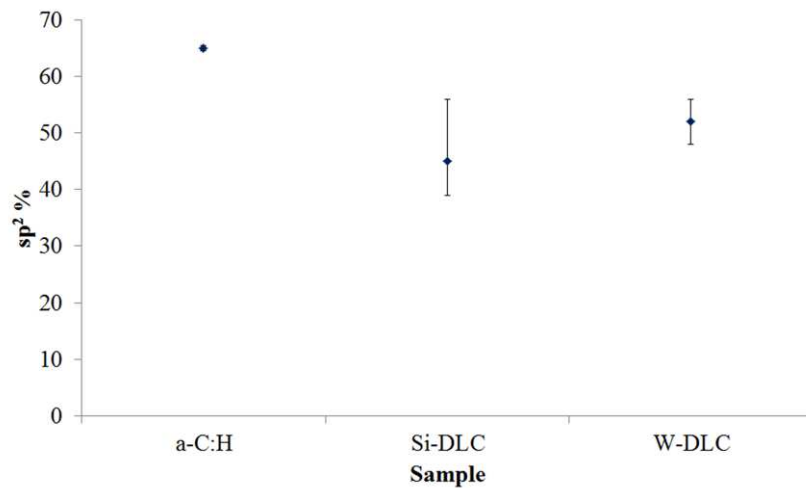


Figure 3-2: Percentage of sp^2 bonded carbon determined by the electron energy loss spectroscopy analysis of a-C:H, Si-DLC and W-DLC

3.3. Wear

Tribological testing was carried out on all of the samples using a pin-on-reciprocating-plate tribometer described earlier. The tests were carried out for durations of 6 and 20 hours,

corresponding to a sliding distance of 432 m and 1440 m respectively. Each experiment was repeated three times to ensure reliability and repeatability of results. The wear coefficient of each of the samples can be seen in figure 3-3. It is clear from these results that the a-C:H sample tested in fully formulated oil + ZDDP had a lower wear coefficient than the Si-DLC, and significantly less than the W-DLC, in both base oil and fully formulated oil + ZDDP.

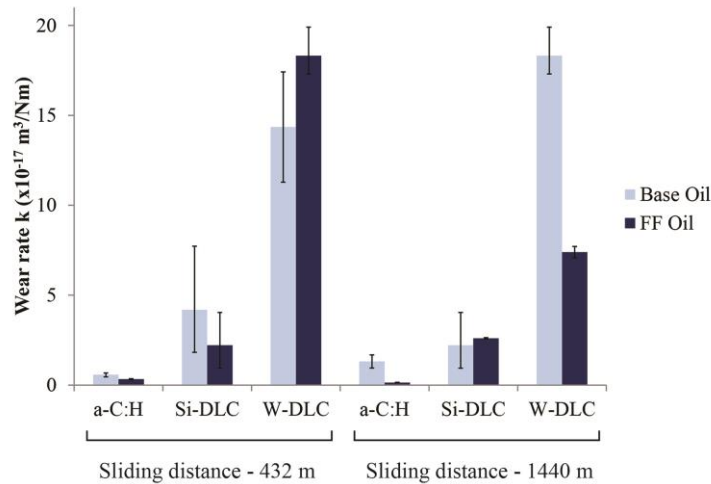


Figure 3-3: Wear rate for a-C:H, Si-DLC and W-DLC sliding against cast iron counter body in base oil and fully formulated oil + ZDDP (FF oil) for a distance of 432 and 1440 m

Figure 3-4 shows white light interferometer images of the a-C:H, Si-DLC and W-DLC wear scars after 20 hours in fully formulated oil + ZDDP. As can be seen from these images, the a-C:H shows signs of mild wear, the Si-DLC shows more severe wear and the W-DLC more so, having been completely removed.

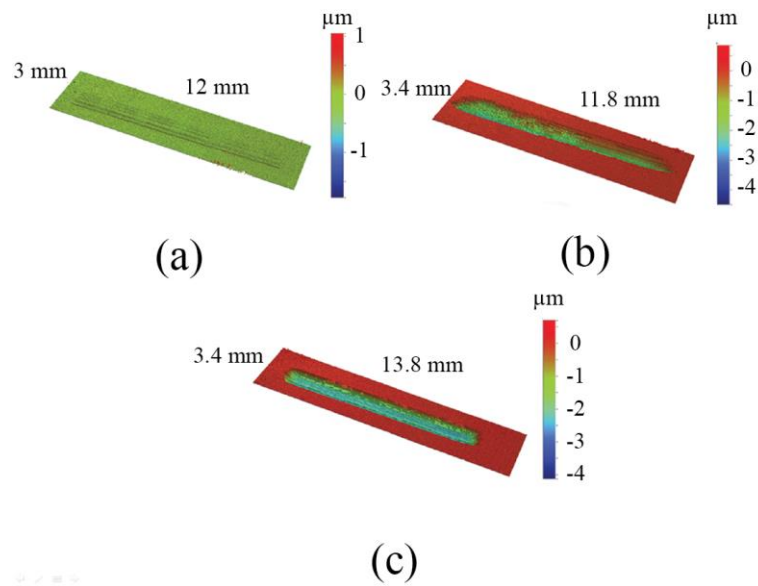


Figure 3-4: White light interferometry images for (a) a-C:H, (b) Si-DLC and (c) W-DLC after testing on pin on reciprocating plate tribometer for twenty hours in fully formulated oil + ZDDP

Figure 3-5 presents the friction coefficient as a function of the wear rate of the Si doped and a-C:H plates. It can be seen here that the coatings which performed with the lowest friction and wear values were the a-C:H coatings in both base oil and fully formulated oil. The coefficient of friction taken for these values is the steady state friction which was taken as the friction value averaged over the last hour of each test. The W-DLC coatings were not included due to the friction and wear values not being representative of the coating because of its complete removal in both tests, thus showing that this particular formulation of W-DLC is not suitable for this application.

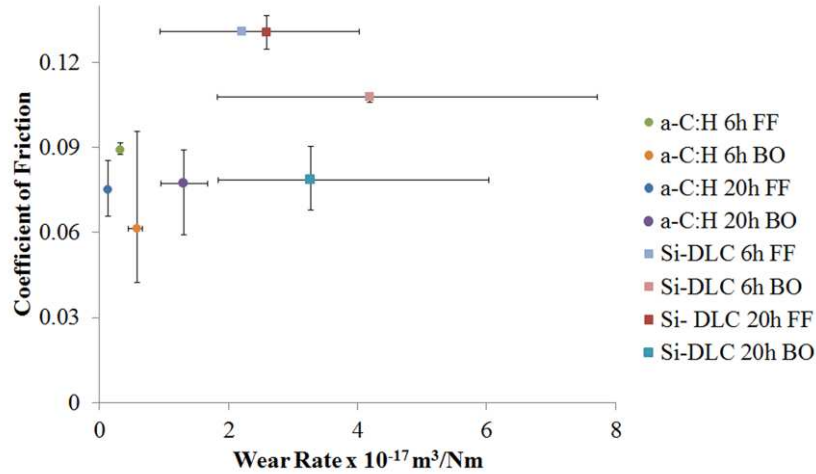


Figure 3-5: Coefficient of friction as a function of wear rate for a-C:H, Si-DLC and W-DLC tested in base oil (BO) and fully formulated oil + ZDDP (FF) for 6 and 20 h

3.4. Counter body wear

Figure 3-6 shows the corresponding counter body wear for the coatings shown in the previous section. The counter body sliding against a-C:H is seen to have a consistently low wear rate, with W-DLC being the highest. Si-DLC outperforms a-C:H in base oil after 6 hours (432 m) only. The wear rate for the Si-DLC and W-DLC coatings are higher in when tested in fully formulated oil than in base oil. This is possibly due to an adverse reaction with the silicon and tungsten dopants within the oil which has been reported by other authors [28], however some authors present an improvement in wear rates when the DLC incorporates silicon [29].

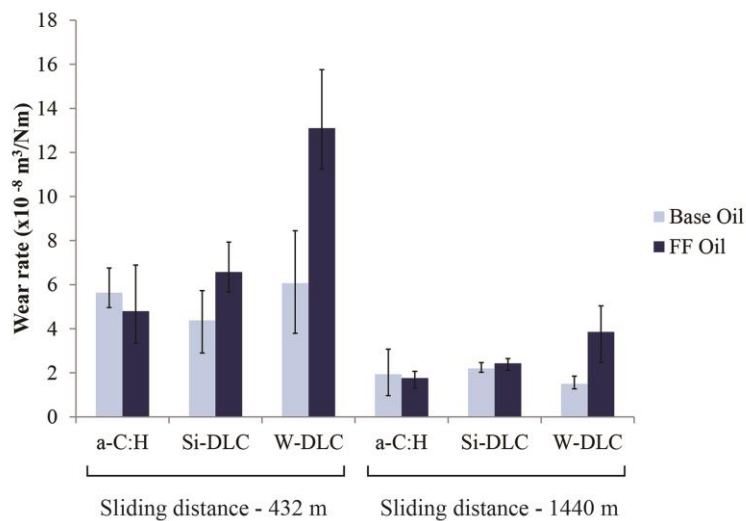


Figure 3-6: Wear rate for cast iron counter bodies sliding against a-C:H, Si-DLC and W-DLC in base oil and fully formulated oil + ZDDP (FF oil) for 432 and 1440 m.

3.5. Atomic Force Microscopy

After the tribometer testing, it was apparent that the W-DLC did not perform well after complete coating removal within the wear scar, and as such was discontinued from further testing. The a-C:H and Si-DLC sample surfaces were inspected using a VEECO AFM before and after tribological testing, these images can be seen in figure 3-7, figure 3-8 and figure 3-9 respectively.

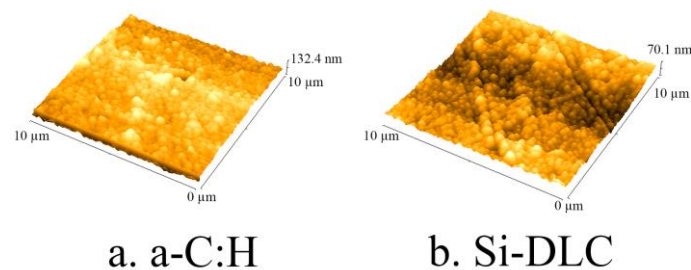


Figure 3-7: Atomic force microscopy images of a-C:H and Si-DLC prior to tribological testing

It can be seen in the AFM images in figure 3-8 that the a-C:H tested for 6 hours is relatively unaffected by the sliding when tested in fully formulated oil. When the same test is conducted in base oil, there are obvious signs of severe polishing wear. The Si-DLC in the AFM images in figure 3-9 tested for 6 hours in base oil also shows signs of severe polishing wear. The test conducted for Si-DLC in fully formulated oil begins to show signs of wear, as can be seen by the directionality of the wear track beginning to form.

The AFM images shown for the testing conducted for 20 hours in fully formulated oil + ZDDP are shown for a-C:H and Si-DLC in figure 3.8 d and figure 3-9 d respectively. Each of the images shows evidence of a tribofilm, though the patchy like structure is more evident in the a-C:H image. The images show evidence of different wear mechanisms; the Si-DLC shows signs of polishing wear and some directional wear, also coating removal, which is indicated by the depth of the coating loss during these tests being equivalent to the coating thickness. The a-C:H was protected by what appears in the AFM images to be a tribofilm, the Si-DLC appears to have a similar structure, but since the tribo-testing showed severe removal

of the Si-DLC, it was not continued to the further X-Ray Photoelectron Spectroscopy (XPS) testing.

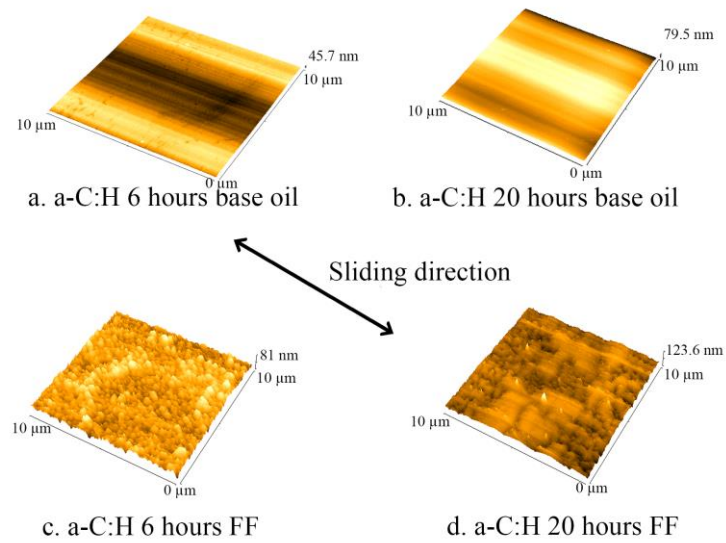


Figure 3-8: Atomic force microscopy images of a-C:H after testing on pin-on-reciprocating plate tribometer for (a) 6 h in base oil, (b) 20 h in base oil, (c) 6 h in fully formulated oil and (d) 20 h in fully formulated oil

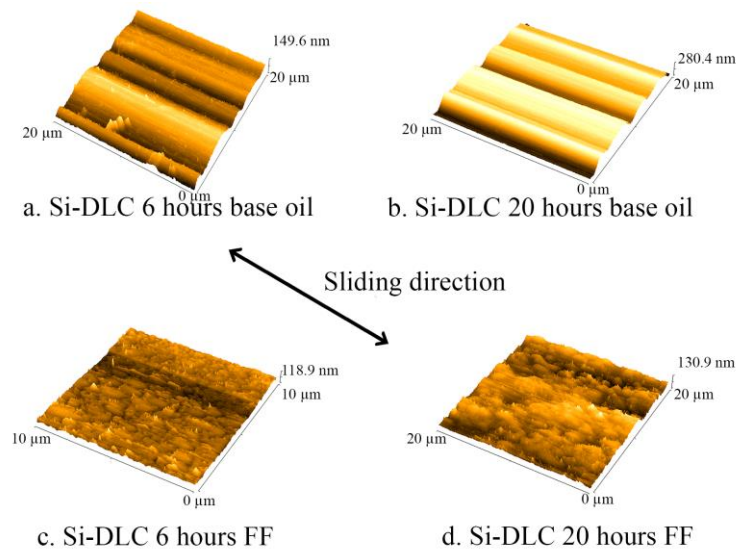


Figure 3-9: Atomic force microscopy images of Si-DLC after testing on pin on reciprocating plate tribometer for (a) 6 h in base oil, (b) 20 h in base oil, (c) 6 h in fully formulated oil and (d) 20 h in fully formulated oil

3.6. XPS

X-ray Photoelectron Spectroscopy was carried out on the a-C:H sample alone; since the Si-DLC sample had been partially removed during the tribometer testing and showed little signs of a tribofilm in the AFM analysis, it was not included. The W-DLC sample was not included due to the severe coating removal experienced by this coating during tribo-testing.

XPS analysis was carried out on the cast iron counter body and the a-C:H sample after tribo-testing on a pin on reciprocating plate tribometer for 6 and 20 hours in fully formulated oil containing ZDDP, results of this can be seen in table 3-2 and table 3-3, respectively.

It is apparent that tribofilm species are present on both the pin and plate as early as 6 hours, as is evidenced by the presence of zinc, phosphorus and oxygen as phosphate components detected on the surface by the XPS, shown in table 3-2 and table 3-3. The phosphorus peak at 133.7 eV, present on the a-C:H plate after 6 hours testing is typically associated with a glassy phosphate, and is the typical structure for a ZDDP tribofilm [20].

In the 20 hours XPS results, the O1s peak shows a binding energy of 532.1 eV on the a-C:H surface, and 531.9 eV on the cast iron counter body surface, which is typically associated with phosphates and sulphates. After curve fitting the S 2p peak in both samples, it was found that this element exists in both samples as a sulphide [30], rendering the O bonding to be that of a phosphate, which can be attributed to the phosphate tribofilm theorised to form. The O 1s peak corresponds to Fe_2O_3 in the cast iron counter body, alongside the Fe 2p peak; this is known to react with the ZDDP in the lubricant to form a glassy phosphate tribofilm.

Table 3-2: Binding energies and chemical species found using XPS of the ZDDP derived tribofilm found on the DLC surface and that of the cast iron counter body after 6 hours of testing on pin-on-reciprocating plate tribometer.

Sample	Element	Binding Energy	Relative Amount of Species
a-C:H after 6 hour tribometer test	O 1s	531.9	Phosphate/Sulphate (41%)
		532.9	Phosphate (59%)
	S 2p	163	Sulphide (100%)
		P 2p	133.5
	134.5		Metaphosphate (59%)
	Zn 2p	1022.9	ZnS/ZnO/Zn-Phosphate (100%)
Cast Iron Counter Body After 6 hour tribometer test	O 1s	531.4	Phosphate/Sulphate (88%)
		533.2	C-O Compound (12%)
	S 2p	160.8	Sulphide (21%)
		161.9	Sulphide (79%)
	P 2p	132.9	Pyrophosphate (51%)
		133.8	Pyrophosphate (49%)
	Zn 2p	1022	ZnS/ZnO/Zn-Phosphate (100%)
Fe 2p	710.8	Fe ₂ O ₃	
	711.9	(100%)	

Table 3-3: Binding energies and chemical species found using XPS of the ZDDP derived tribofilm found on the DLC surface and that of the cast iron counter body after 20 hours of testing on pin-on-reciprocating plate tribometer.

Sample	Element	Binding Energy	Relative Amount of Species
a-C:H after 20 hours tribometer test	O 1s	532.1	Phosphate/Sulphate (100%)
	S 2p	160.9	Sulphide (10.5%)
		162.3	Sulphide (89.5%)
	P 2p	133.6	Pyrophosphate (66.67%)
		134.4	Metaphosphate (33.33%)
Zn 2p	1022.6	ZnS/ZnO/Zn-Phosphate (100%)	
Cast Iron Counter Body After 20 hours tribometer test	O 1s	529.9	Fe ₂ O ₃ (9.87%)
		531.7	Phosphate/Sulphate (90.13%)
	S 2p	161.1	Sulphide (20.89%)
		162.2	Sulphide (79.11%)
	P 2p	133.1	Pyrophosphate (66.67%)
		133.9	Pyrophosphate (33.33%)
	Zn 2p	1022.1	ZnS/ZnO/Zn-Phosphate (100%)
	Fe 2p	710.9	Fe ₂ O ₃

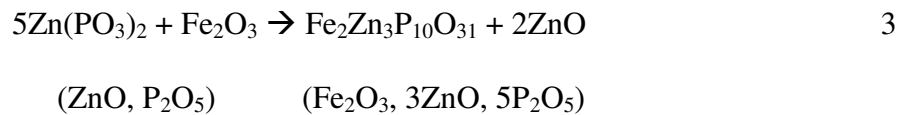
4. Discussion

The mechanical properties of three Diamond-Like Carbon coatings deposited using plasma enhanced chemical vapour deposition (a-C:H, Si-DLC and W-DLC) have been determined and evaluated, alongside their tribological performance in two different oils; a group III base oil, and a fully formulated oil with a group III base stock containing the anti-wear additive ZDDP. The coatings will be compared with those in the literature, and the mechanisms of formation of a phosphate tribofilm will be discussed.

4.1. Tribochemical Interactions

ZDDP is commonly used as an anti-wear additive in boundary lubrication conditions. The protection mechanisms for ZDDP in a ferrous environment are well documented. Nascent iron and iron oxide wear debris generated during sliding form an integral part of phosphate film formation as described by some authors [31], [32], whereas others describe the formation as a purely thermally induced process [33].

The formation of a phosphate film is based in the HSAB (hard and soft (Lewis) acid base theory). Phosphates (in this case a polymer-like zinc meta-phosphate) derived from ZDDP are defined as ‘hard base’ and will react strongly with the hard acid (Fe^{3+}) from the cast iron pins.



Equation 3 shows the cation exchange process between Fe_2O_3 and ZnO (as described by [32]). The digestion of the iron oxide in the phosphate glass protects the surface from wear; this process requires friction to generate the iron oxide particles. As the wear protection of the surface becomes more prevalent and Fe is no longer being worn from the surface of the cast iron pin, more negative charges are needed to balance the exchange of Zn^{2+} with Fe^{3+} . Thus the chain length of the long metaphosphates is shortened into pyrophosphates in order to provide the negative charges. This phosphate tribofilm is dynamic in that once the iron oxide particles are provided, the protection is sufficient to no longer need them, in which case the tribofilm has formed short pyrophosphates which protect the surface further; acting as ‘molten’ glass and allowing localised EHL (elastohydrodynamic lubrication) sites to occur on the surface of the sample.

4.1.1. a-C:H

Within this study, it is apparent that a glassy phosphate film has been discovered on the surface of both the a-C:H DLC sample and the cast iron counter body after 6 and 20 hours of testing on the tribometer. It is proposed that the phosphate present in the additive has reacted with the Fe_2O_3 in the cast iron counter body as described above. It is then seen to transfer to

the DLC surface during sliding, since this surface is inert and doesn't react with the ZDDP [34, 35]. The XPS results of the quantified chemical species shown after tribo-testing for 6 and 20 hours table 3-2 and table 3-3, respectively, show that the phosphate present after 6 hours is mostly long chained Metaphosphate (59%), after 20 hours of testing, the shorter pyrophosphate chains dominate at a concentration of 67%. In the cast iron counter body, the phosphate occurs as short chain pyrophosphate (100%) after both 6 and 20 hours testing. It is seen in the literature that short chained pyrophosphate derived from the ZDDP anti-wear additive is more effective in protecting the surfaces than the long chain metaphosphates [36]. This suggests that the film transferred to the DLC surface changes from long chained metaphosphates to short chain pyrophosphates at a slower rate, or that it is transferred gradually from the cast iron pin to the DLC. On the cast iron pin, the metaphosphate was not detected by XPS. The change to pyrophosphate here is much faster and thus protects the surface from an earlier stage.

The gradual transfer of the phosphate tribofilm to the surface of DLC is supported by other results; the wear rate of the a-C:H coating decreases over time, as is shown in figure 3-3 suggesting this gradual build up. The AFM images presented in figure 3-8 show a clear tribofilm present on the a-C:H surface after 20 hours, however this cannot be seen on the 6 hour sample image. This could be due to the tribofilm being too thin for the AFM to detect on the sample tested for 6 hours, since the XPS results presented in table 3-2 and table 3-3 show species on the surface of both samples tested at 6 and 20 hours, respectively, that are present in the classic ZDDP tribofilm, this shows that a tribofilm of this nature is indeed present after both 6 and 20 hours.

A much thicker tribo layer is seen in the AFM images for the a-C:H after 20 hours, it is suggested that due to the presence of the tribofilm as proven by the XPS data, the wear rate decreasing and wear volume remaining static, that the tribofilm is formed initially on the cast iron counter body surface and is gradually transferred to the a-C:H surface during sliding, eventually providing protection of this surface.

4.1.2. Si-DLC

The Si-DLC did not perform as well as the a-C:H in the tribometer tests with regards to wear rate, shown in figure 3-3. The Si-DLC shows signs of coating removal from 6 hours in base

oil, and the coating was completely removed in some areas after 20 hours of testing. In the fully formulated oil a similar trend was also seen. After 6 hours, some signs of coating removal were present; however, this was less severe than in the tests conducted in base oil. In the white light interferometer images seen after 20 hours testing in figure 3-4 it can be seen that some areas of the coating were completely removed, with some areas surrounding this that show signs of coating removal, but not wholly. In the areas where the coating remained, some protection may have been present - a possible tribofilm as seen in the AFM images in figure 3-9 - but any protection offered by the tribofilm had been negated as the coating had worn away faster than the tribofilm could build up. The wear mechanism is suggested to originally be that of adhesion, but after the coating begins to wear away, a third body interaction appears to be taking place which exacerbates removal of the coating.

4.1.3. W-DLC

The W-DLC coating was completely removed in each of the tribometer tests. This is evident from the wear rate. The wear rate values are an order of magnitude higher than those experienced by the a-C:H coating in base oil. This increase in wear for this type of coating has been noted in the literature. Kalin et al. [37] discovered recently that W-DLC did not perform well within a sliding environment in base oil or in a fully formulated oil with anti-wear and extreme pressure additives. The W-DLC failure is attributed to severe adhesive wear and mutual transfer of coating and counter body species, causing an alteration in coating structure and the decomposition of the W-DLC, forming complex carbides (η -phase W_6-xFe_xC). The drop in wear rate of the W-DLC seen in figure 3-3 at first glance seems promising, this is due to there being no coating left to wear through, and over time the wear rate appears lower. However, when the samples were analysed using white light interferometry, it was clear that the wear rate had decreased due to the coating being fully removed, and there being no material left to wear through. It has been suggested by Vengudusamy et al. [28] that wear induced graphitisation can inhibit the formation of the distinctive phosphate pad like structure, which is typically formed by the ZDDP additive, this mechanism could be inhibiting tribofilm formation within this study as seen in both the W-DLC and Si-DLC samples.

4.2. Friction

The steady state friction for Si-DLC and a-C:H are presented in base oil in figure 4-1 and in fully formulated oil + ZDDP in figure 4-2. Friction was seen to be affected by the ZDDP additive. Primarily an anti-wear additive, ZDDP was not expected to affect the friction in a large way. However, it was noticed in the a-C:H coating that friction indeed decreased over time, whereas the Si-DLC stayed consistent.

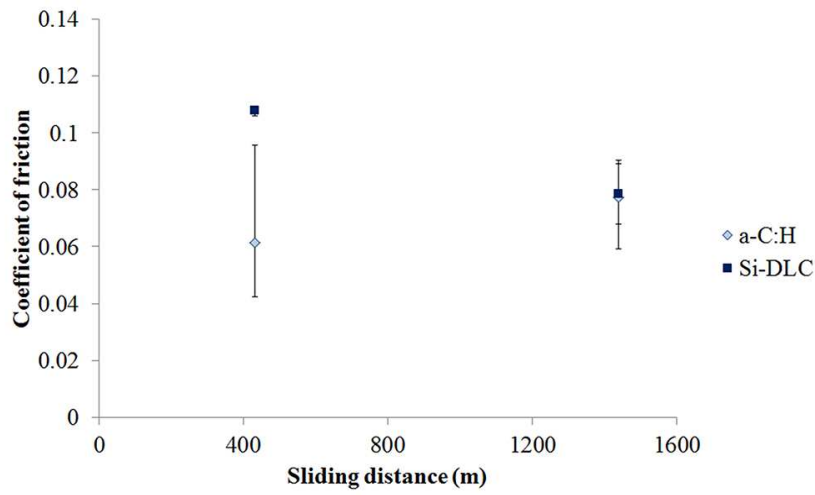


Figure 4-1: Steady state friction for a-C:H and Si-DLC tested on pin on reciprocating plate tribometer in base oil

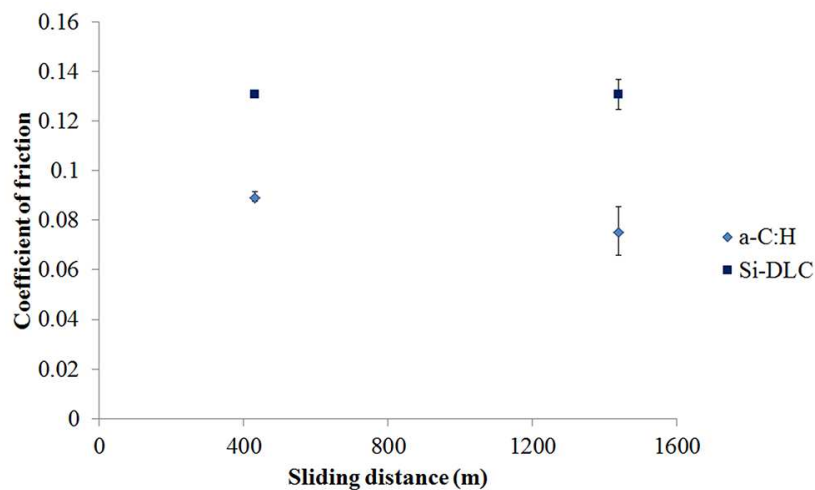


Figure 4-2: Steady state friction for a-C:H and Si-DLC tested on pin on reciprocating plate tribometer in fully formulated oil + ZDDP

The experiments conducted in base oil in both a-C:H and Si -DLC show the friction to be unstable and quite unrepeatable, giving large error bars and in the case of Si-DLC, partial removal of the coating. The results in fully formulated oil + ZDDP are similar to those found by Vengudusamy et al. [28], showing that friction is minimally affected by the ZDDP additive. The Si-doped DLC tested in base oil had a decreasing steady state friction over time, whereas in the fully formulated oil + ZDDP, the steady state friction increased over time. In both instances of lubrication, the Si-DLC coating had been removed at 20 hours testing; the presence of the ZDDP in the lubricant appears to increase the friction once coating removal has occurred, whereas in base oil this is reduced. The W-DLC experienced an increase in friction coefficient in both the base oil and the fully formulated oil + ZDDP, which again agrees with the results of Vengudusamy et al. [28], however, unlike the results in this study, the coating had been completely removed by this time and therefore the friction measured was largely that between the substrate and the counter body, rather than the coating and the counter body.

4.3. Friction and wear

The coefficient of friction as a function of wear rate is presented in figure 3-5. W-DLC was again excluded due to complete coating removal, therefore the friction value given being unrepresentative of that between the coating and the counter body. It is apparent that the combination of a-C:H and the fully formulated oil + ZDDP was the most successful in terms of the lowest wear rate and friction coefficient. The samples tested in base oil were very unstable with regards to friction and show high error due to this. The a-C:H sample performed better in both base oil and fully formulated oil + ZDDP, showing less friction and wear than the Si-DLC tested in fully formulated oil. This could be due to the a-C:H being harder than the Si-DLC, this property of the a-C:H could afford it higher wear resistance and lower friction. Also the synergy of the coating and the counter body with the ZDDP additive is clearly contributing to both the friction and wear resistance. The best coating and lubricant combination for these tests are indicated in the lower left hand side in figure 3-5 with regards to low friction and wear.

The wear rate of the a-C:H samples is shown as a function of the coating hardness in figure 4-3 and compared with those found in the literature. The sample was measured to be ~ 3 GPa harder than the Si-DLC; hardness is a property often attributed to increased wear resistance

[38] and it is clear that this property has an impact in this instance, since even in the samples tribo-tested in base oil, the wear rate is lower in the harder sample (a-C:H) than of the Si-DLC, which is of lower hardness as indicated in figure 4-3.

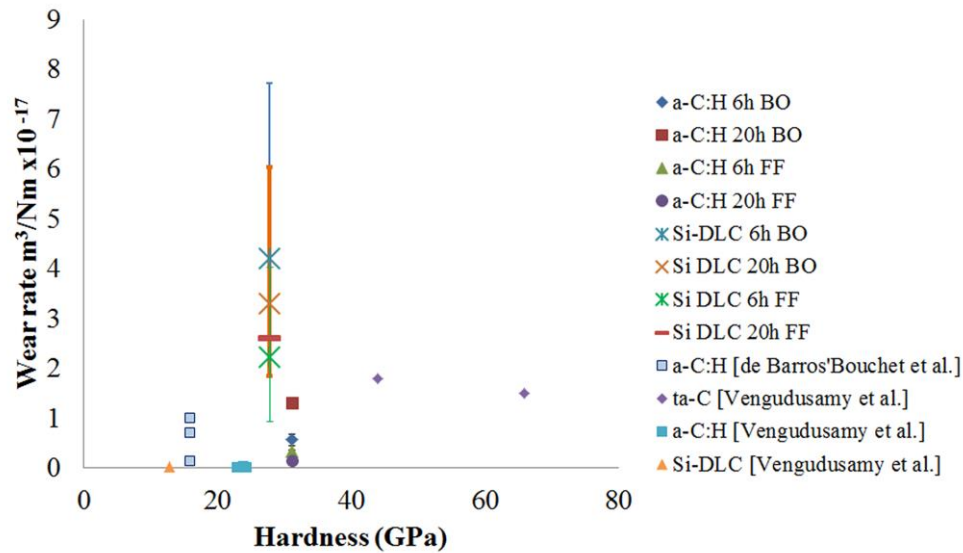


Figure 4-3: Wear rate as a function of coating hardness of a-C:H and Si-DLC. BO = Base oil, FF = Fully formulated oil + ZDDP

There is much debate in the literature surrounding the prediction of a coatings wear lifetime using varying means. Figure 4-4 presents the wear rate (after 20 hours of testing in base oil (BO) and fully formulated (FF) oil) as a function of the critical load taken from scratch tests for a-C:H, Si-DLC and W-DLC. This shows that as the critical load increases, as does the wear rate of the sample. This was surprising due to the critical load being a measure of a materials scratch resistance, but as is evidenced by figure 4-4, a higher scratch resistance does not necessarily equate to a higher wear resistance, in fact, the opposite appears to be true. The scratch testing takes place at room temperature and involves no lubrication, thus the softer coating (W-DLC) will have the opportunity to deform elastically, whereas the other, harder samples (with higher elastic modulus) do not. Bull *et al.* [39] performed a comparison on the wear resistance of TiN coatings to the scratch resistance and found the two to positively correlate, however these tests were conducted using no lubrication and thus the tribochemistry of the coatings were not under consideration. The H/E ratio of each of the samples is presented in table 3-1, the H/E ratio is sometimes used by authors as a tool to predict wear performance of coatings and other materials [26] which is said to indicate the

materials elastic strain to failure, with a higher value of H/E being more conducive to a higher wear resistance. Of the three samples tested in this study, the W-DLC had the highest H/E ratio, signifying that it should have the best wear resistance. This was untrue for the samples tested in lubricant on the tribometer, however, the W-DLC sample outperformed both the a-C:H and Si-DLC on the scratch tests, reaching a critical load of 56.5 N, as opposed to that reached by a-C:H and Si-DLC of 31.4 N and 35.72 N respectively. It would seem that the wear resistance indicated by the H/E ratio was true for the dry scratch tests, but both of these values were not useful in predicting wear resistance in lubricated contacts, which have a more complicated tribochemistry, as can be seen from figure 4-4.

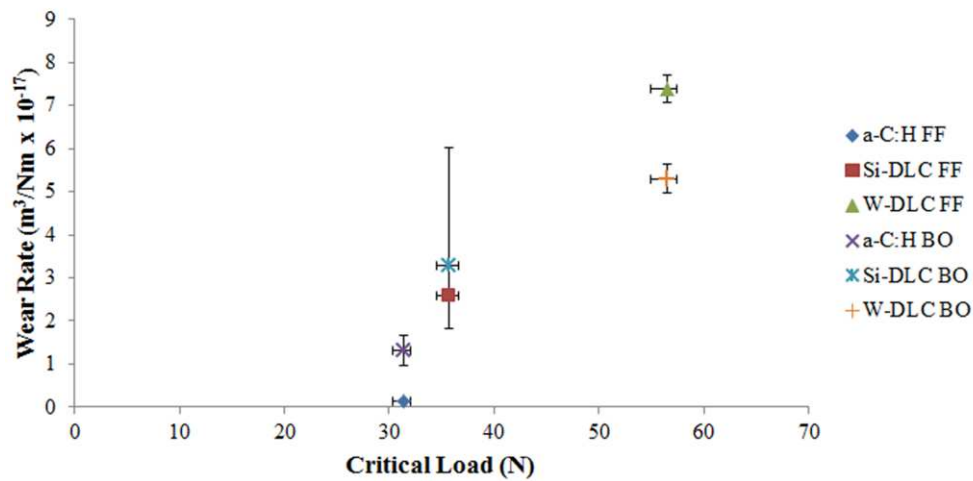


Figure 4-4: Wear rate as a function of critical load for a-C:H, Si-DLC and W-DLC after 20 h testing.

5. Conclusions

The following conclusions can be made from this study:

- It has been shown that ZDDP has an effect on the wear resistance of a-C:H coating surfaces when reciprocating against a cast iron counter body
- A phosphate based tribofilm has been produced on the a-C:H surfaces
- The phosphate tribofilm on the a-C:H surface has been shown to consist mainly of long chained metaphosphates after 6 hours sliding against a cast iron pin, devolving into short chained pyrophosphates after twelve/20 hours.

- It has been shown that the short chained pyrophosphates enhances the protection of the a-C:H surface more so than the short chained metaphosphates.
- The phosphate film is transferred from the cast iron pin to the a-C:H surface over time.
- ZDDP was seen to lower the friction minimally in the case of a-C:H
- The Si-DLC used within this study was not adequate for the application due to coating removal during testing.
- A tribofilm was seen to begin to form on the Si-DLC surface, but the removal of the coating preceded this, negating any protection it could potentially offer.
- The W-DLC (Balanit C*) proved completely unsuitable for this application, being completely removed from the substrate after 6 hours of testing.
- The H/E ratio is seen to be a helpful indicator of the samples' scratch resistance.

References

- [1] R. Hauert, "A review of modified DLC coatings for biological applications," *Diamond and Related Materials*, vol. 12, pp. 583-589, 2003.
- [2] R. Hauert, "An overview on the tribological behavior of diamond-like carbon in technical and medical applications," *Tribology International*, vol. 37, pp. 991-1003, 2004.
- [3] J. Robertson, "Comparison of diamond-like carbon to diamond for applications," *Physica Status Solidi (a)*, vol. 205, pp. 2233-2244, 2008.
- [4] P. A. Dearnley, "Coatings tribology drivers for high density plasma technologies," *Surface Engineering*, vol. 26, pp. 80-96, 2010.
- [5] C. Donnet and E. Erdemir, *Tribology of Diamond-Like Carbon Films. Fundamentals and Applications*. New York: Springer Science, 2008.
- [6] S. V. Hainsworth and N. J. Uhure, "Diamond like carbon coatings for tribology: production techniques, characterisation methods and applications," *International Materials Reviews*, vol. 52, pp. 153-174, 2007.
- [7] S. D. A. Lawes, S. V. Hainsworth, and M. E. Fitzpatrick, "Impact wear testing of diamond-like carbon films for engine valve-tappet surfaces," *Wear*, vol. 268, pp. 1303-1308, 2010.
- [8] A. Grill, "Diamond-like carbon: state of the art," *Diamond and Related Materials*, vol. 8, pp. 428-434, 1999.
- [9] K. Holmberg and A. Matthews, *Coatings tribology: properties, mechanisms, techniques and applications in surface engineering*: Elsevier Science, 2009.
- [10] C. Donnet, "Recent progress on the tribology of doped diamond-like and carbon alloy coatings: a review," *Surface and Coatings Technology*, vol. 100 - 101, pp. 180-186, 1998.
- [11] A. Grill, "Review of the tribology of diamond-like carbon," *Wear*, vol. 168, pp. 143-153, 1993.
- [12] A. Grill, "Tribology of diamondlike carbon and related materials: an updated review," *Surface and Coatings Technology*, vol. 94-95, pp. 507-513, 1997.
- [13] J. Robertson, "Amorphous carbon," *Advances in Physics*, vol. 35, pp. 317-374, 2013/08/12 1986.
- [14] A. Erdemir, "Friction and wear of diamond and diamond-like carbon films," *Proceedings of the Institution of Mechanical Engineers, Part J: Journal of Engineering Tribology*, vol. 216, pp. 387-400, 2002.
- [15] A. Erdemir and C. Donnet, "Tribology of diamond-like carbon films: recent progress and future prospects," *Journal of Physics D: Applied Physics*, vol. 39, p. R311, 2006.

- [16] G. Dearnaley and J. H. Arps, "Biomedical applications of diamond-like carbon (DLC) coatings: A review," *Surface and Coatings Technology*, vol. 200, pp. 2518-2524, 2005.
- [17] J. Robertson, "Diamond-like amorphous carbon," *Materials Science and Engineering: R: Reports*, vol. 37, pp. 129-281, 2002.
- [18] T. Haque, A. Morina, and A. Neville, "Influence of friction modifier and antiwear additives on the tribological performance of a non-hydrogenated DLC coating," *Surface and Coatings Technology*, vol. 204, pp. 4001-4011, 2010.
- [19] T. Haque, A. Morina, A. Neville, R. Kapadia, and S. Arrowsmith, "Effect of oil additives on the durability of hydrogenated DLC coating under boundary lubrication conditions," *Wear*, vol. 266, pp. 147-157, 2009.
- [20] T. e. a. Haque, "Study of the ZDDP Antiwear Tribofilm Formed on the DLC Coating Using AFM and XPS Techniques," *Journal of ASTM International*, vol. 4, 2006.
- [21] B. Podgornik, D. Hren, and J. Vizintin, "Low-friction behaviour of boundary-lubricated diamond-like carbon coatings containing tungsten," *Thin Solid Films*, vol. 476, pp. 92-100, 2005.
- [22] B. Podgornik, S. Jacobson, and S. Hogmark, "DLC coating of boundary lubricated components - Advantages of coating one of the contact surfaces rather than both or none," *Tribology International*, vol. 36, pp. 843-849, 2003.
- [23] W. C. Oliver and G. M. Pharr, "An improved technique for determining hardness and elastic modulus using load and displacement sensing indentation experiments," *Journal of Materials Research*, vol. 7, pp. 1564-1583, 1992.
- [24] H. Daniels, R. Brydson, B. Rand, and A. Brown, "Investigating carbonization and graphitization using electron energy loss spectroscopy (EELS) in the transmission electron microscope (TEM)," *Philosophical Magazine*, vol. 87, pp. 4073-4092, 2007.
- [25] J. F. Moulder, W. F. Stickle, P. E. Sobol, and K. D. Bromben, *Handbook of X-ray Photoelectron Spectroscopy*. USA: Perkin-Elmer Corporation, 1992.
- [26] A. Leyland and A. Matthews, "On the significance of the H/E ratio in wear control: a nanocomposite coating approach to optimised tribological behaviour," *Wear*, vol. 246, pp. 1-11, 2000.
- [27] X. Jiang, K. Reichelt, and B. Stritzker, "The hardness and Young's modulus of amorphous hydrogenated carbon and silicon films measured with an ultralow load indenter," *Journal of Applied Physics*, vol. 66, pp. 5805-5808, 1989.
- [28] B. Vengudusamy, J. H. Green, G. D. Lamb, and H. A. Spikes, "Influence of hydrogen and tungsten concentration on the tribological properties of DLC/DLC contacts with ZDDP," *Wear*, vol. 298-299, pp. 109-119, 2013.
- [29] J. Lanigan, H. Zhao, A. Morina, and A. Neville, "Tribochemistry of silicon and oxygen doped, hydrogenated Diamond-like Carbon in fully-formulated oil against low additive oil," *Tribology International*, vol. Article in press, 2014.

- [30] T. Haque, "Tribiochemistry of Lubricant Additives on Non-Ferrous Coatings for Reduced Friction, Improved Durability and Wear in Internal Combustion Engines," Ph.D Thesis, School of Mechanical Engineering, University of Leeds, Leeds, 2007.
- [31] G. W. Stachowiak, *Wear: Materials, Mechanisms and Practice*: John Wiley and Sons, 2005.
- [32] J. Martin, "Antiwear mechanisms of zinc dithiophosphate: a chemical hardness approach," *Tribology Letters*, vol. 6, pp. 1-8, 1999.
- [33] M. L. S. Fuller, M. Kasrai, G. M. Bancroft, K. Fyfe, and K. H. Tan, "Solution decomposition of zinc dialkyl dithiophosphate and its effect on antiwear and thermal film formation studied by X-ray absorption spectroscopy," *Tribology International*, vol. 31, pp. 627-644, 1998.
- [34] T. Haque, A. Morina, A. Neville, R. Kapadia, and S. Arrowsmith, "Non-ferrous coating/lubricant interactions in tribological contacts: Assessment of tribofilms," *Tribology International*, vol. 40, pp. 1603-1612, 2007 2007.
- [35] H. Renondeau, R. I. Taylor, G. C. Smith, and A. A. Torrance, "Friction and wear performance of diamond-like carbon and Cr-doped diamond-like carbon coatings in contact with steel surfaces," *Proceedings of the Institution of Mechanical Engineers, Part J: Journal of Engineering Tribology*, vol. 222, pp. 231-240, 2008.
- [36] M. Crobu, A. Rossi, and N. Spencer, "Effect of Chain-Length and Countersurface on the Tribiochemistry of Bulk Zinc Polyphosphate Glasses," *Tribology Letters*, vol. 48, pp. 393-406, 2012.
- [37] M. Kalin and J. Vizintin, "Differences in the tribological mechanisms when using non-doped, metal-doped (Ti, WC), and non-metal-doped (Si) diamond-like carbon against steel under boundary lubrication, with and without oil additives," *Thin Solid Films*, vol. 515, pp. 2734-2747, 2006.
- [38] R. C. D. Richardson, "The wear of metals by relatively soft abrasives," *Wear*, vol. 11, pp. 245-275, 1968.
- [39] S. J. Bull, "Can scratch testing be used as a model for the abrasive wear of hard coatings?," *Wear*, vol. 233-235, pp. 412-423, 12// 1999.